Kinetic and Mechanistic Study of OH- and Cl-Initiated Oxidation of Two Unsaturated HFCs: $C_4F_9CH{=}CH_2$ and $C_6F_{13}CH{=}CH_2$

E. Vésine, V. Bossoutrot, A. Mellouki,* G. Le Bras, J. Wenger,† and H. Sidebottom‡

LCSR/CNRS-1C, Avenue de la recherche scientifique, 45071, Orléans Cedex 2, France

Received: April 6, 2000; In Final Form: June 16, 2000

The kinetics and mechanisms of the OH- and Cl-initiated oxidation of two unsaturated HFCs, $C_4F_9CH{=}CH_2$ and $C_6F_{13}CH{=}CH_2$, were investigated. The kinetic study was performed as a function of pressure and temperature for the OH reactions and as a function of pressure at 298 K for Cl atom reactions. The rate constants obtained are (in units of cm^3 $molecule^{-1}$ s^{-1}): $k(OH + C_4F_9CH{=}CH_2) = (8.5 \pm 1.4) \times 10^{-13}$ $\exp[(139 \pm 48)/T]$ and $k(OH + C_6F_{13}CH{=}CH_2) = (1.3 \pm 0.5) \times 10^{-12}$ $\exp[(31 \pm 124)/T]$ in the temperature range 233−372 K; and $k(Cl + C_4F_9CH{=}CH_2) = (8.9 \pm 1.0) \times 10^{-11}$ and $k(Cl + C_6F_{13}CH{=}CH_2) = (9.1 \pm 1.0) \times 10^{-11}$ at 298 K. The OH and Cl reactions rate constants were found to be independent of pressure in the range 10−760 and 15−60 Torr, respectively. The mechanistic study was performed in air at atmospheric pressure, in the presence or absence of NO_x. CO and COF_2 have been identified as the major secondary products of both OH- and Cl-initiated oxidation of the HFCs. However, there is evidence for the formation of different primary products: aldehydes (C_4F_9CHO and $C_6F_{13}CHO$) in the OH oxidation of the HFCs and ketones ($C_4F_9C(O)CH_2Cl$ and $C_6F_{13}C(O)CH_2Cl$) in the Cl oxidation. This suggests that the oxy radicals, precursors of these carbonyl compounds, behave differently. The β-hydroxyoxy radicals $C_4F_9CH(O)CH_2OH$ and $C_6F_{13}CH(O)CH_2OH$ decompose, whereas the β-chlorooxy radicals $C_4F_9CH(O)CH_2Cl$ and $C_6F_{13}CH(O)CH_2Cl$ react with O_2. These results are consistent with the significantly higher activation barrier for the decomposition of the β-chlorooxy, compared to that of the β-hydroxyoxy radicals.

Introduction

The legislated phase out of chlorofluorocarbons (CFCs) has led to the use of substitutes, mainly hydrochlorofluorocarbons (HCFCs) and hydrofluorocarbons (HFCs). These hydrogen-containing compounds react with the OH radicals in the troposphere by an H-atom transfer mechanism. The resulting lower atmospheric lifetimes compared to the CFCs make these compounds more acceptable as alternatives. HCFCs are less efficient than CFCs in depleting stratospheric ozone. The effect of these chlorine-containing molecules is, however, not totally negligible and they are also planned to be phased out in the near future. HFCs, which do not contain chlorine, have no effect on stratospheric ozone but they strongly absorb infrared radiation and they may then contribute to the greenhouse effect. The global warming potential of a compound will depend on its capacity to absorb infrared radiation in the atmospheric window (770−1430 cm^{-1}) and on its atmospheric lifetime. The overall atmospheric impact of such compounds may also depend on the fate and impact of their oxidation products. The tropospheric chemistry of the saturated HFCs is mainly controlled by reaction with OH radicals while for the unsaturated ones the contribution of NO_3 and O_3 reactions might be not negligible. The oxidation by Cl atoms is likely to be negligible, considering the presently estimated low Cl atom concentration in the troposphere. However, chlorine atom oxidation in laboratory experiments can provide additional information which can help in defining the atmospheric oxidation of HFC and other organic compounds.

In this paper, we report the first kinetic and mechanistic study of OH and Cl reactions with two unsaturated HFCs: $C_4F_9CH{=}CH_2$ and $C_6F_{13}CH{=}CH_2$. The mechanistic studies were performed in the presence and absence of NO_x.

Experimental Section

The rate constants for the reactions of OH radicals with the two unsaturated HFCs have been measured using the pulsed laser photolysis−laser-induced fluorescence (PLP-LIF) method. The rate constants for reactions of Cl atoms have been determined using pulsed laser photolysis−resonance fluorescence. The studies of the oxidation mechanisms were carried out in a photoreactor coupled with FTIR analysis of the reactants and products.

Pulsed Laser Photolysis−Laser-Induced Fluorescence (PLP-LIF). The PLP-LIF technique and the methodology used have been already described in detail previously (e.g., ref 1) and is only briefly discussed here. Two sources were used to generate OH radicals: photolysis of H_2O_2 at $\lambda = 248$ nm (KrF excimer laser) and photolysis of HONO at $\lambda = 351$ nm (XeF excimer laser). This has been done in order to check the possible complications arising from the photolysis wavelength. The concentration of OH radicals was monitored at various reaction times ranging from 10 μs to 10 ms by pulsed LIF. A Nd:YAG-pumped frequency-doubled dye laser was used to excite the OH radicals at $\lambda = 282$ nm. Fluorescence from the OH radicals was detected by a photomultiplier fitted with a 309 nm narrow band-pass filter. The integrated signals from 10 to 15 delay times from 100 probe laser shots were averaged to generate OH concentration−time profiles over at least three lifetimes.

* Corresponding author. E-mail: mellouki@cnrs-orleans.fr.
† Department of Chemistry, University College, Cork, Ireland.
‡ Department of Chemistry, University College, Dublin, Ireland.

10.1021/jp0013199 CCC: $19.00
Published on Web 08/26/2000

Pulsed Laser Photolysis−Resonance Fluorescence (PLP-RF). This experimental setup as well as the methodology used to measure chlorine atom reaction rate constants have also been already described in previous papers from our group (e.g., ref 2). Briefly, chlorine atoms were produced by photolyzing Cl_2 at 355 nm using a pulsed, frequency tripled, Nd:YAG laser operated at 10 Hz. The radiation ($\lambda \sim 135$ nm) from a microwave discharge in a flowing mixture of (0.2−0.3%) Cl_2/helium at ∼2 Torr pressure was used to excite the fluorescence of Cl atoms in the reactor. A solar blind photomultiplier tube perpendicular to both the resonance lamp and photolysis laser beam collected the resonance fluorescence radiation resulting from excitation of Cl. Signals were obtained using photon-counting techniques in conjunction with multichannel scaling. The decay curves following 10 000−40 000 laser pulses were co-added to improve the signal-to-noise ratio.

Photoreactor. Product studies were performed at UCD-Dublin using the experimental setup described elsewhere.[3] Reactions were carried out in FEP Teflon cylindrical reaction vessel with a volume of about 50 L surrounded by 10 lamps (Philips, TL 20W/09) with irradiation in the range 300−460 nm and a maximum intensity at 365 nm for photolysis of Cl_2 to generate Cl atoms and 10 lamps (Philips, TUV 15W, $\lambda =$ 254 nm) for photolysis of H_2O_2 to generate OH radicals. Measured amounts of reagents were flushed from calibrated bulbs into the Teflon bag by a stream of ultrapure air (Air Liquide). The photoreactor was then filled to its full capacity with ultrapure air. A Mattson Polaris FTIR spectrometer was used for analysis. FTIR spectra were obtained by using an evacuable 2 L Teflon-coated cell containing a multipass White mirror arrangement which was mounted in the cavity of the spectrometer. Spectra were recorded using a 6 m path length over the wavelength range 500−4000 cm^{-1} with a resolution of 2 cm^{-1}. The spectra were derived from 64 co-added spectra.

Materials. Purities of the chemicals were as follows: helium, the carrier gas (UHP certified to >99.9995% (Alphagaz)), was passed from the tank to the cell through a liquid nitrogen trap; Cl_2 (99.8%, UCAR) was degassed several times at 77 K before use; O_2 was certified to >99.995% (Alphagaz). The 50 wt % H_2O_2 solution obtained from Prolabo was concentrated by bubbling helium through the solution to remove water for several days prior to use, and constantly during the course of the experiments. It was admitted into the reaction cell by passing a small flow of helium through a glass bubbler containing H_2O_2. HONO was produced in situ by reacting $NaNO_2$ (0.1 M) with dilute H_2SO_4 (10%) contained in a stirred round-bottomed flask. The effluent from the flask was swept into the cell by a known flow of helium. $C_4F_9CH{=}CH_2$ and $C_6F_{13}CH{=}CH_2$ were from Elf Atochem and their purities were higher than 96.5% and 97%, respectively. The analyzed impurities in the HFCs samples were shown to consist of fluorinated alkanes.

Results and Discussion

Kinetic Studies. ***OH Reaction Rate Constant Measurements***. Reactions were studied under pseudo-first-order conditions with the OH concentration much lower than that of the HFCs ($[OH]_0 = (0.2-2) \times 10^{11}$ molecules cm^{-3}). Thus, the OH concentration time profile followed the pseudo-first-order rate law:

$$[OH]_t = [OH]_0 e^{-k't}; \quad k' = k[HFC] + k'_0$$

where k is the rate coefficient for the reaction OH + HFC. The decay rate, k'_0, is the first-order OH decay rate in the absence of the HFC; it is the sum of the reaction rate of OH with its precursor (H_2O_2 or HONO, with concentrations in the range $(2-10) \times 10^{13}$ molecules cm^{-3}), and the diffusion rate of OH out of the detection zone. k'_0 was typically around 100 s^{-1}.

TABLE 1: OH + $C_4F_9CH{=}CH_2$ Reaction: Experimental Conditions and Measured Rate Constants

T (K)	P (Torr)	$[C_4F_9CH{=}CH_2]$ (10^{14} molecules cm^{-3})	$k' - k'_0$ (s^{-1})	$(k \pm 2\sigma) \times 10^{12}$ (cm^3 $molecule^{-1}$ s^{-1})
372	100	3.49−20.28	645−2736	1.27 ± 0.03
	100	3.56−20.83	726−2961	1.33 ± 0.16[a]
	100	4.65−22.38	485−2818	1.29 ± 0.10[a]
343	100	2.04−21.74	467−2875	1.26 ± 0.03
323	100	2.06−23.15	470−3086	1.27 ± 0.02
	100	5.16−21.06	660−2924	1.35 ± 0.09[a]
298	300	5.94−66.45	793−8475	1.25 ± 0.06
	200	2.33−24.63	626−3485	1.31 ± 0.02
	100	2.28−28.42	477−3804	1.28 ± 0.01
	100	2.93−33.60	549−4480	1.30 ± 0.02
	50	5.09−55.88	1206−7610	1.27 ± 0.02
	10	1−12.28	1419−3011	1.25 ± 0.04
	100	3.94−28.80	427−3973	1.44 ± 0.06[a]
	100	5.80−32.42	715−4462	1.33 ± 0.10[a]
	50	8.96−35.72	1085−4395	1.41 ± 0.07[a]
273	100	2.44−27.02	509−3808	1.34 ± 0.02
	100	1.89−35.97	436−5389	1.46 ± 0.08[a]
253	100	2.76−32.78	628−4930	1.43 ± 0.01
	20	1.99−22.07	1401−4348	1.56 ± 0.04
	100	7.69−38.61	1069−5875	1.55 ± 0.08[a]
233	100	3.67−42	725−6633	1.54 ± 0.03
	100	7.19−40.03	934−5469	1.63 ± 0.09[a]

[a] Experiments performed with HONO as source of OH.

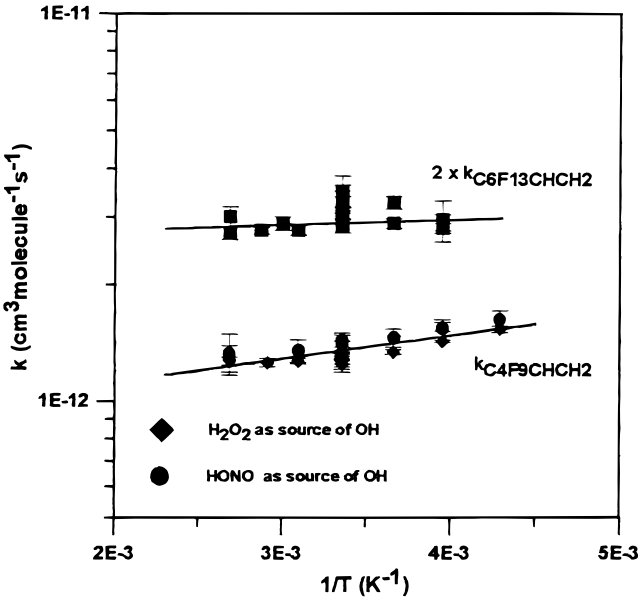

Figure 1. Arrhenius expression of the rate constants for the reactions of OH with $C_4F_9CH{=}CH_2$ and $C_6F_{13}CH{=}CH_2$.

The experiments were performed in the pressure ranges 10−300 Torr at 298 K and 20−100 Torr at 253 K. No pressure dependence of the reaction rate constant was observed in these ranges. Changes in the experimental conditions (photolysis laser fluence by a factor of 2, and flow velocity by a factor of 3) did not affect the obtained data. The Arrhenius expression derived from the unweighted least-squares fit to the combined results

Reaction OH + $C_4F_9CH{=}CH_2$. The reaction of OH with $C_4F_9CH{=}CH_2$ was studied over the temperature range 233−372 K using H_2O_2 or HONO as the OH source. The obtained data were similar with the two sources as shown in Table 1 and Figure 1.

TABLE 2: OH + $C_6F_{13}CH{=}CH_2$ Reaction: Experimental Conditions and Measured Rate Constants

T (K)	P (Torr)	$[C_6F_{13}CH{=}CH_2]$ (10^{14} molecules cm^{-3})	$k' - k'_0$ (s^{-1})	$(k \pm 2\sigma) \times 10^{12}$ (cm^3 molecule^{-1} s^{-1})
372	100	0.7−8.72	105−1178	1.36 ± 0.05
	100	0.93−8.95	115−1315	1.50 ± 0.09
348	100	0.69−9.31	105−1267	1.38 ± 0.03
333	100	1.06−10.65	119−1514	1.44 ± 0.06
323	100	0.78−10.05	106−1380	1.38 ± 0.04
298	760	8.28−37.31	1020−5056	1.35 ± 0.11
	400	1.77−20.93	180−2506	1.22 ± 0.05
	300	1.35−19.76	138−2293	1.18 ± 0.04
	100	0.84−8.91	65−1345	1.50 ± 0.03
	100	0.83−9.80	111−1353	1.42 ± 0.06
	100	0.69−7.50	111−1232	1.61 ± 0.08
	50	0.62−8.59	104−1137	1.33 ± 0.03
	20	0.36−5.07	122−672	1.36 ± 0.14
	100	0.74−8.07	129−1321	1.65 ± 0.10[a]
	100	0.64−7.09	125−1130	1.73 ± 0.18[a]
	100	0.82−8.62	130−1259	1.51 ± 0.07[a]
	100	1.01−9.38	167−1482	1.61 ± 0.08[a]
	100	0.65−7.83	83−1261	1.70 ± 0.11[a]
273	100	0.94−14.61	134−1906	1.44 ± 0.04
	100	0.91−9.64	121−1573	1.63 ± 0.06
253	100	1.47−16.53	233−2203	1.45 ± 0.07
	100	1−10.90	137−1742	1.47 ± 0.18
	100	1.22−12.81	207−1773	1.40 ± 0.04

[a] Experiments performed in the presence of O_2.

obtained with the two OH sources in the temperature range 233−372 K is

$$k(\mathrm{OH}+\mathrm{C_4F_9CH{=}CH_2}) = (8.5 \pm 1.4) \times 10^{-13} \exp[(139 \pm 48)/T]\ \mathrm{cm^3\ molecule^{-1}\ s^{-1}}$$

The uncertainties for the preexponential factor, A, and the activation energy are given by $\Delta A = 2A\sigma_{\ln A}$ and $\Delta E/R = 2\sigma_{E/R}$.

The room temperature rate constant taken as the average of all values obtained at 298 K is

$$k(\mathrm{OH}+\mathrm{C_4F_9CH{=}CH_2}) = (1.3 \pm 0.2) \times 10^{-12}\ \mathrm{cm^3\ molecule^{-1}\ s^{-1}}$$

The uncertainty represents the statistical one to which we have added 10% for systematic errors.

Reaction OH + $C_6F_{13}CH{=}CH_2$. The rate constant for this reaction was determined over the temperature range 253−372 K using H_2O_2 as the OH source (Table 2).

At 298 K, measurements were carried out in the pressure range 20−760 Torr. Several experiments were also performed in the presence of O_2 (P_{O_2} = 3−7 Torr) at 100 Torr. At 298 K, the data obtained at different pressures and in the presence or absence of O_2 were similar. The following value

$$k(\mathrm{OH}+\mathrm{C_6F_{13}CH{=}CH_2}) = (1.5 \pm 0.3) \times 10^{-12}\ \mathrm{cm^3\ molecule^{-1}\ s^{-1}}$$

represents the average of the combined data obtained at room temperature. The measured rate constants are shown plotted in Arrhenius form in Figure 1. The Arrhenius expression derived from the experimental data between 253 and 372 K is

$$k(\mathrm{OH}+\mathrm{C_6F_{13}CH{=}CH_2}) = (1.3 \pm 0.5) \times 10^{-12} \exp[(31 \pm 124)/T]\ \mathrm{cm^3\ molecule^{-1}\ s^{-1}}$$

Uncertainties are calculated similarly to that for $k(\mathrm{OH}+\mathrm{C_4F_9CH{=}CH_2})$.

TABLE 3: Experimental Conditions and the Measured Rate Constant Data for the Cl Reaction with $C_4F_9CH{=}CH_2$ and $C_6F_{13}CH{=}CH_2$

molecule	P (Torr)	[HFC] × 10^{-12} (molecules cm^{-3})	$k' - k'_0$ (s^{-1})	$k \times 10^{11}$ (cm^3 molecule^{-1} s^{-1})
$C_4F_9CH{=}CH_2$	60	6.0−53.3	542−4437	8.9 ± 1.0
	15	4.7−49.0	392−3890	
$C_6F_{13}CH{=}CH_2$	60	6.9−65.11	606−5867	9.1 ± 1.0
	15	4.1−47.02	365−3948	

Discussion. The present rate constant data are the first to be reported for OH reactions with long-chain fluoroalkenes. However, these results can be compared with the existing data on the OH reactions with smaller fluoroalkenes such as fluoroethenes and fluoropropenes. Recently, Orkin and al.[4] reported rate constants data for the reaction of OH with CF_3-$CH{=}CH_2$, $CF_3CF{=}CH_2$, and $CF_3CF{=}CF_2$. Their data showed that the reaction of OH with $CF_3CH{=}CH_2$ (1.5×10^{-12} cm^3 molecule^{-1} s^{-1}) is more than 1 order of magnitude slower at 298 K than the reaction of OH with $CH_3CH{=}CH_2$ (26.3×10^{-12} cm^3 molecule^{-1} s^{-1}). This was attributed to the presence of the strongly electron-withdrawing CF_3- group. Our data shows that the substitution of CF_3- by the larger fluorinated groups C_4F_9- or C_6F_{13}- does not lead to a significant change in the rate constants at 298 K ($k = 1.5 \times 10^{-12}$, 1.3×10^{-12}, 1.5×10^{-12} cm^3 molecule^{-1} s^{-1} for $CF_3CH{=}CH_2$, $C_4F_9CH{=}CH_2$, and C_6F_{13}-$CH{=}CH_2$, respectively). These C_4F_9- and C_6F_{13}- groups have essentially the same deactivating effect as CF_3-. In a manner similar to the simple alkenes, the reactions of OH with fluorenated alkenes have a small negative temperature factor, E/R, which is consistent with an addition of OH to the double bond of the alkenes. However, it is interesting to note that the E/R factor for OH reaction with $CH_3CH{=}CH_2$ (−504 K) is lower than that with $CF_3CH{=}CH_2$, $C_4F_9CH{=}CH_2$, and C_6F_{13}-$CH{=}CH_2$ (−183, −139, and −31 K, respectively).

Cl Reaction Rate Constant Measurements. The chlorine atom reactions with the two HFCs were also studied under pseudo-first-order conditions with the Cl concentration much lower than that of the HFCs. Thus, the Cl concentration time profile followed the pseudo-first-order rate law:

$$[\mathrm{Cl}]_t = [\mathrm{Cl}]_0 e^{-k't}; \quad \text{where } k' = k[\mathrm{HFC}] + k'_0$$

k is the rate coefficient for the reaction of Cl with HFC. The decay rate, k'_0, is the first-order Cl decay rate in the absence of the HFC; it is the diffusion rate of Cl out of the detection zone. The measurements were performed at 298 ± 2 K and at two different pressures, 15 and 60 Torr of helium. The obtained rate constants are

$$k(\mathrm{Cl}+\mathrm{C_4F_9CH{=}CH_2}) = (8.9 \pm 1.0) \times 10^{-11}\ \mathrm{cm^3\ molecule^{-1}\ s^{-1}}$$

$$k(\mathrm{Cl}+\mathrm{C_6F_{13}CH{=}CH_2}) = (9.1 \pm 1.0) \times 10^{-11}\ \mathrm{cm^3\ molecule^{-1}\ s^{-1}}$$

independent of pressure between 15 and 60 Torr. The experimental conditions together with the values of the rate constants are presented in Table 3, and shown in Figure 2.

Discussion. Rate constants $k(\mathrm{Cl}+\mathrm{C_4F_9CH{=}CH_2})$ and $k(\mathrm{Cl}+\mathrm{C_6F_{13}CH{=}CH_2})$ are equal within the experimental errors.

Comparison of the rate constant data for the reactions of Cl atoms with the unsaturated HFCs determined in this work, with the reported rate constant of reaction Cl + $CH_3CH{=}CH_2$ (k= 2×10^{-10} cm^3 molecule^{-1} s^{-1} at 298 K for the addition channel),[5] indicates that the C_4F_9- and C_6F_{13}- groups have a

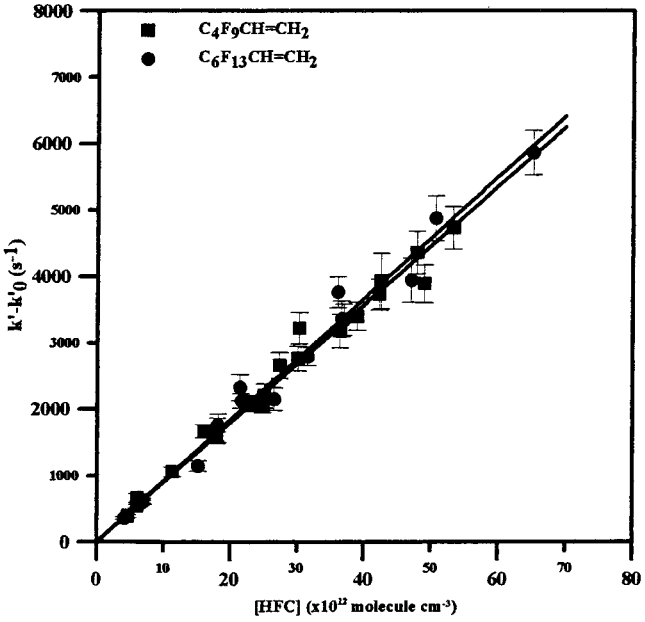

Figure 2. Reactions of Cl with $C_4F_9CH=CH_2$ and $C_6F_{13}CH=CH_2$: plots of $(k' - k'_0)$ versus $C_4F_9CH=CH_2$ and $C_6F_{13}CH=CH_2$ concentrations at 298 K.

significant deactivation effect with respect to reaction with Cl atoms as observed for the OH reactions but lower. The deactivation effect is not as pronounced as for the analogous reactions with OH radicals. This is the consequence that reactions of Cl atoms are much faster and then have a much narrower range of rate constants than the OH reactions.

Mechanistic Studies. The oxidation of the two unsaturated HFCs was initiated by either OH radicals or Cl atoms in air in the absence or presence of NO_x. Preliminary experiments showed that photolysis at 254 or 365 nm contributed to less than 1% per hour in the consumption of the two HFCs.

Mechanism of the OH-Initiated Oxidation of $C_4F_9CH=CH_2$. *(a) In the Absence of NO_x.* Experiments were performed by irradiation of $C_4F_9CH=CH_2/H_2O_2$/air mixtures at 254 nm. Five independent experiments were conducted where the initial concentrations of $C_4F_9CH=CH_2$ were in the range 20−90 ppm. An example of obtained FTIR spectra before irradiation and after 60 min of irradiation of the mixture is given in Figure 3.

The identified reaction products were CO, COF_2, and HC(O)OH. In addition, after subtraction of the spectra of the products CO, COF_2, and HC(O)OH, and also $C_4F_9CH=CH_2$, an absorption band between 1830 and 1730 cm^{-1} was observed and attributed to the carbonyl function (C=O) of $C_4F_9C(O)H$ similarly to that of $C_6F_{13}C(O)H$ which has been produced in an independent experiment by the photolysis of a mixture of $C_6F_{13}CH=CH_2/Cl_2$/air (see next section). The residual spectrum also shows a series of bands between 1400 and 1100 cm^{-1} which correspond to C−F bonds of C_4F_9.

The observed plots of CO, COF_2, and $C_4F_9C(O)H$ concentrations versus $C_4F_9CH=CH_2$ consumed (Figure 4) indicate that CO and COF_2 are secondary products while the fluorinated aldehyde is a primary product of the reaction. A primary product is defined as a product whose formation is rate limited by the initial OH reaction with the HFCs, while for a secondary product, the formation is rate limited by the reaction of a primary product.

The following mechanism is suggested to explain these observations. The primary step of the OH reaction with $C_4F_9CH=CH_2$ is an electrophilic addition of OH to the double bond and predominantly to the terminal carbon. The yield of this addition channel is expected to be higher than 65% which is the yield of the similar channel of the OH + propene addition reaction.[6] This hypothesis is based on the strong electron-

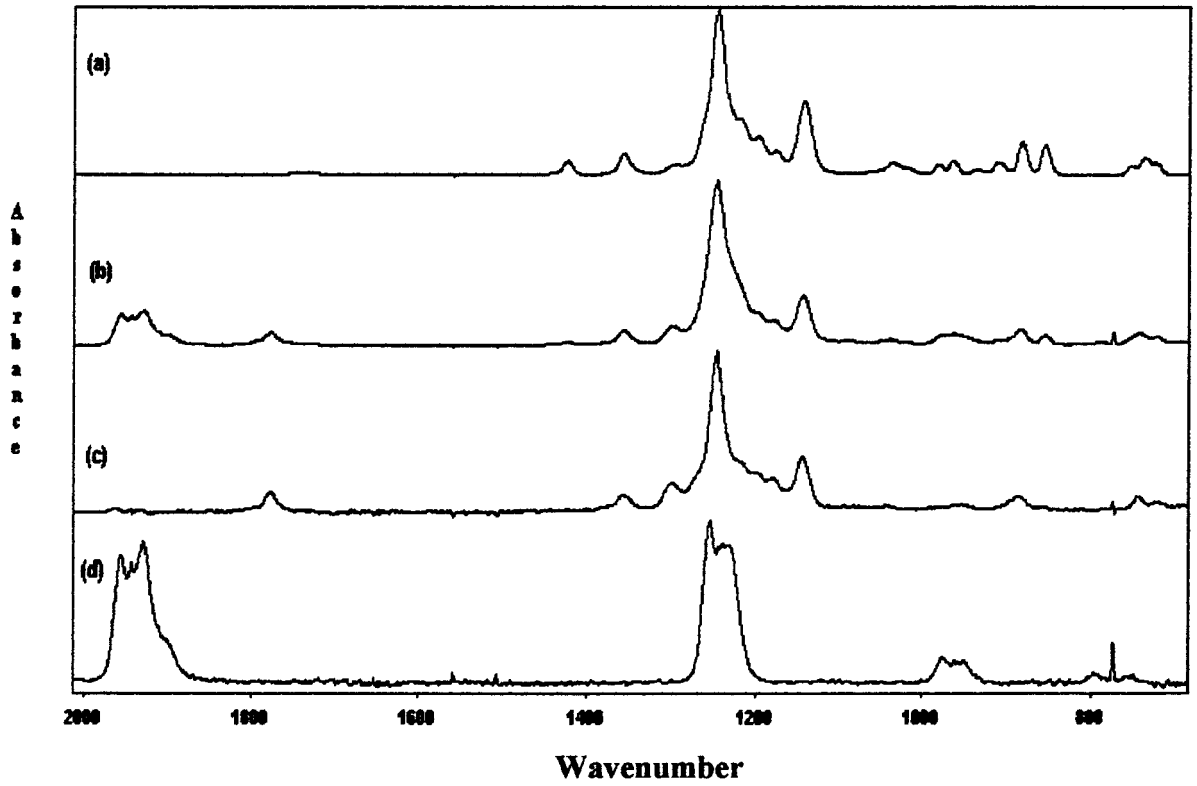

Figure 3. FTIR spectra for the OH + $C_4F_9CH=CH_2$ reaction in air in the absence of NO_x: **(a)** spectrum of $C_4F_9CH=CH_2$ before irradiation, **(b)** spectrum after 60 min irradiation, **(c)** spectrum of $C_4F_9C(O)H$ after subtraction of $C_4F_9CH=CH_2$,COF_2, CO and HC(O)OH, and **(d)** reference spectrum of COF_2. Absorbance is in arbitrary units.

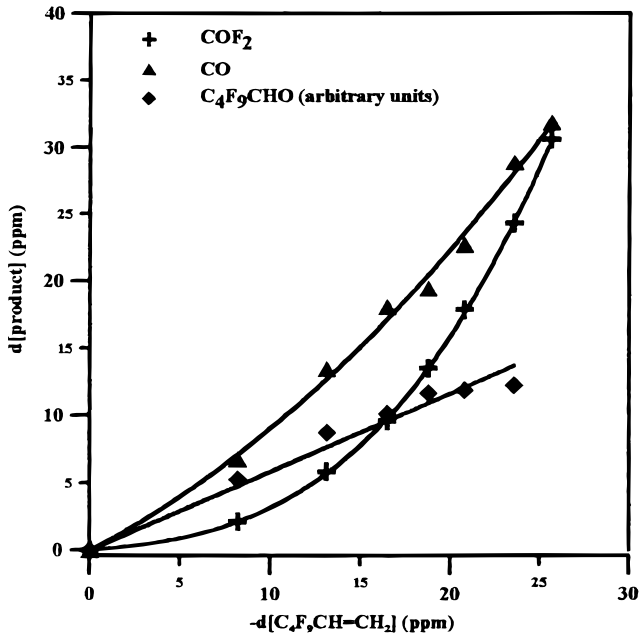

Figure 4. Concentrations of products versus consumption of $C_4F_9CH{=}CH_2$ in the OH-oxidation of $C_4F_9CH{=}CH_2$ in the absence of NO_x, in air, $[C_4F_9CH{=}CH_2]_o = 30$ ppm.

withdrawing effect of the C_4F_9 group which is expected to reduce the electron density on the adjacent carbon of the double bond in $C_4F_9CH{=}CH_2$ more than that of the terminal carbon. Therefore, in air, the following initial mechanism is expected:

$$OH + C_4F_9CH{=}CH_2 + M \rightarrow C_4F_9CHCH_2OH + M \quad (1)$$

$$C_4F_9CHCH_2OH + O_2 + M \rightarrow C_4F_9CH(OO)CH_2OH + M \quad (2)$$

In absence of NO_x, the self-combination peroxy radical produced can proceed through the two following channels:

$$C_4F_9CH(OO)CH_2OH + C_4F_9CH(OO)CH_2OH \rightarrow 2C_4F_9CH(O)CH_2OH + O_2 \quad (3a)$$

$$\rightarrow C_4F_9C(O)CH_2OH + C_4F_9CH(OH)CH_2OH + O_2 \quad (3b)$$

The oxy radical formed in reaction 3a can decompose by carbon−carbon bond fission or react with O_2:

$$C_4F_9CH(O)CH_2OH + M \rightarrow C_4F_9C(O)H + CH_2OH + M \quad (4)$$

$$C_4F_9CH(O)CH_2OH + O_2 \rightarrow C_4F_9C(O)CH_2OH + HO_2 \quad (5)$$

The observation of $C_4F_9C(O)H$ and not that of $C_4F_9C(O)CH_2OH$ indicates that the reaction proceeds through channel 3a followed by channel 4. The other possible decomposition channel:

$$C_4F_9CH(O)CH_2OH + M \rightarrow C_4F_9 + HC(O)CH_2OH + M \quad (6)$$

was considered to be unimportant since features corresponding to a pure spectrum of glycolaldehyde, $HC(O)CH_2OH$, was not observed in the FTIR spectrum of the products. The CH_2OH radical also formed in reaction 4 will react with O_2 to produce HCHO:

$$CH_2OH + O_2 \rightarrow HCHO + HO_2 \quad (7)$$

However, HCHO was not observed since it reacted rapidly with OH. The absolute concentrations of CO and COF_2 were determined using their calibrated reference spectra. This was not possible for $C_4F_9C(O)H$ since its calibrated spectrum was not available. Accounting only for CO, COF_2, and HC(O)OH as reaction products the carbon balance is about 43%. The missing part could be attributed mainly to $C_4F_9C(O)H$. The observed CO and HC(O)OH products are expected to be generated from the oxidation of HCHO.[7] COF_2 is likely to be produced from the aldehyde $C_4F_9C(O)H$ which reacts with OH or photolyses to form C_4F_9 which is a precursor of COF_2:

$$C_4F_9C(O)H + OH \rightarrow C_4F_9CO + H_2O \quad (8a)$$

$$C_4F_9C(O)H + h\nu \rightarrow C_4F_9 + \text{products} \quad (8b)$$

$$C_4F_9CO + O_2 + M \rightarrow C_4F_9C(O)O_2 + M \quad (9)$$

$$C_4F_9CO + M \rightarrow C_4F_9 + CO + M \quad (10)$$

$$C_4F_9C(O)O_2 + C_4F_9C(O)O_2 \rightarrow 2C_4F_9C(O)O + O_2 \quad (11)$$

$$C_4F_9C(O)O + M \rightarrow C_4F_9 + CO_2 + M \quad (12)$$

$$C_4F_9 + O_2 + M \rightarrow C_4F_9O_2 + M \quad (13)$$

$$C_4F_9O_2 + RO_2 \rightarrow C_4F_9O + \text{products} \quad (14)$$

$$C_4F_9O + M \rightarrow C_3F_7 + COF_2 + M \quad (15)$$

$$C_3F_7 + O_2 + M \rightarrow \rightarrow \rightarrow COF_2 \quad (16)$$

CF_3O produced in sequence (16) may partly react with the peroxy radicals $C_nF_{2n+1}O_2$ to produce trioxide $CF_3O_3C_nF_{2n+1}$ since IR bands characteristics of trioxide were probably observed.[8,9] This mechanism, where COF_2 is formed through the $C_4F_9C(O)H$ intermediate, is consistent with the observation of COF_2 as a secondary product.

The relative importance of reactions 8a and 8b in our experiments is not known. However, photolysis of C_4F_9CHO is likely to be slow at the 254 nm wavelength, considering the low absorption cross section of the similar molecule, CF_3CHO, at this wavelength.[10] The reaction of C_4F_9CHO with OH can be significant within the reaction time of the experiment since the concentration−time profile of C_4F_9CHO exhibits a maximum (observed after 1 h of experiment). The rate constant for the reaction of C_4F_9CHO with OH (reaction 8a) is not known but it can be assumed to be equal or less than that for the reaction of CF_3CHO with OH: $k = 6 \times 10^{-13}$ cm^3 molecule^{-1} s^{-1} at 298 K.[11] This lower value compared to that for the initial reaction of $C_4F_9CH{=}CH_2$ with OH can qualitatively explain the concentration−time profiles of C_4F_9CHO.

(b) In the Presence of NO_x. Four experiments were performed in the presence of NO_x with initial concentrations of $C_4F_9CH{=}CH_2$ and NO ranging from 20 to 60 ppm and 15 to 45 ppm, respectively. The major identified products were COF_2 and CO. Subtraction of the known spectra of $C_4F_9CH{=}CH_2$, HC(O)OH, and COF_2 from that obtained after 60 min of irradiation gives a spectrum which indicates the presence of organic nitrate(s) (Figure 5). This latter spectrum clearly shows the characteristics of PAN-like absorption bands at 1841, 1741, 1304, and 790 cm^{-1}. The PAN-like compound is most likely $C_4F_9C(O)O_2NO_2$ produced from the reaction of $C_4F_9C(O)H$ with OH which has been suggested to be the major loss process for

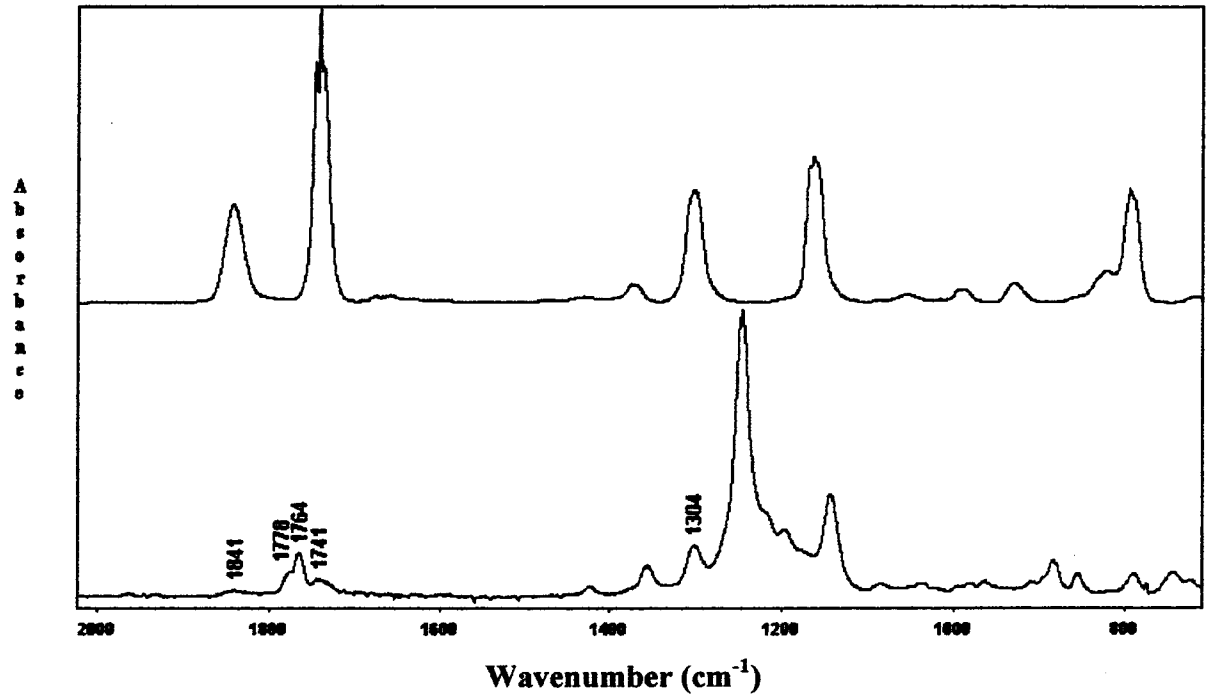

Figure 5. **(a)** Reference spectrum of PAN; **(b)** residual spectrum for the OH + $C_4F_9CH{=}CH_2$ reaction in air, in the presence of NO_x, obtained after 60 min photolysis, after subtraction of $C_4F_9CH{=}CH_2$, HC(O)OH, and COF_2.

$C_4F_9C(O)H$ in our experiments. $C_4F_9C(O)O_2NO_2$ would be produced by reactions 8a, 9, and 17:

$$C_4F_9C(O)O_2 + NO_2 + M \rightarrow C_4F_9C(O)O_2NO_2 + M \quad (17)$$

In the presence of NO_x, $C_4F_9C(O)H$ is also produced by decomposition of the oxy radical $C_4F_9CH(O)CH_2OH$ (reaction 4). But this oxy radical is produced by the following reaction, instead of reaction 3 in the absence of NO_x:

$$C_4F_9CH(OO)CH_2OH + NO \rightarrow C_4F_9CH(O)CH_2OH + NO_2 \quad (18)$$

Besides, the absorption band observed at 1764 cm^{-1} (Figure 5) is likely due to an organic nitrate product like $C_nF_{2n+1}O_2NO_2$, this band having been attributed to $CF_3O_2NO_2$ in previous studies.[12,13]

Mechanism of the Cl-Initiated Oxidation of $C_4F_9CH{=}CH_2$. *(a) In the Absence of NO_x.* Two experiments were conducted with initial concentrations of 40 ppm of the HFC and Cl_2 in air using the TL 20W/09 lamps (irradiation in the range 300−460 nm with a maximum intensity at 365 nm). CO, COF_2, and an unknown species were observed. The obtained concentration profiles of the products versus consumed $C_4F_9CH{=}CH_2$ are shown in Figure 6. The profiles indicate that CO and COF_2 are secondary products of the reaction as for the OH-initiated oxidation of $C_4F_9CH{=}CH_2$ while the "unknown" species is a primary product.

The unknown product has an infrared band at 1788 cm^{-1}, which corresponds to a carbonyl group. However, the corresponding compound is not $C_4F_9C(O)H$, since the band at 1777 cm^{-1} attributed to this species in the OH-initiated oxidation of $C_4F_9CH{=}CH_2$ was not observed in the Cl-initiated oxidation. Besides, the spectra obtained, after subtraction of $C_4F_9CH{=}CH_2$ and COF_2, show features in the region 1400−1100 cm^{-1}, likely due to C−F absorption bands similar to those attributed to $C_4F_9C(O)H$. Then, the unknown product in the Cl-initiated

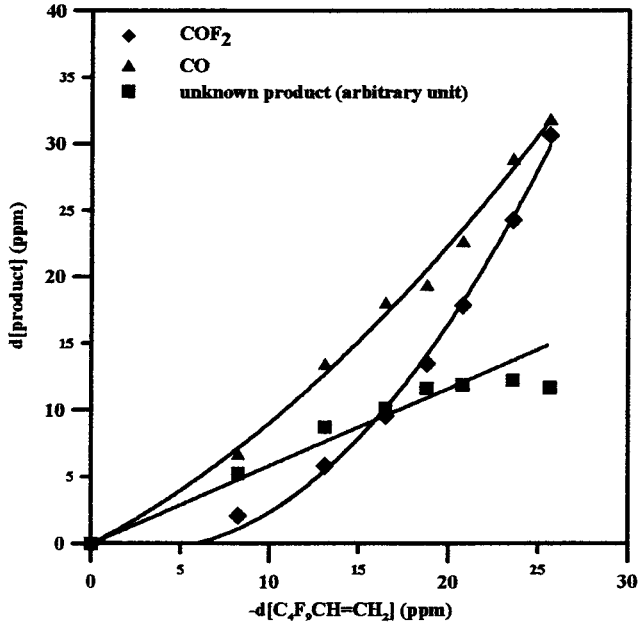

Figure 6. Concentrations of products versus consumption of $C_4F_9CH{=}CH_2$ in the Cl oxidation of $C_4F_9CH{=}CH_2$ in air, in the absence of NO_x. $[C_4F_9CH{=}CH_2]_0$ = 40 ppm.

oxidation of $C_4F_9CH{=}CH_2$ is assumed to be a C_4F_9-containing carbonyl compound other than $C_4F_9C(O)H$.

The following mechanism is proposed to explain the observed products. For the same reason as for the OH reaction, the initial addition channel is expected to occur predominantly at the terminal carbon of the double bond:

$$Cl + C_4F_9CH{=}CH_2 + M \rightarrow C_4F_9CHCH_2Cl + M \quad (19)$$

The peroxy and oxy radical are produced as follows:

$$C_4F_9CHCH_2Cl + O_2 + M \rightarrow C_4F_9CH(OO)CH_2Cl + M \quad (20)$$

$$C_4F_9CH(OO)CH_2Cl + C_4F_9CH(OO)CH_2Cl \rightarrow 2C_4F_9CH(O)CH_2Cl + O_2 \quad (21)$$

The decomposition of the oxy radical, as observed in the OH reaction

$$C_4F_9CH(O)CH_2Cl + M \rightarrow C_4F_9C(O)H + CH_2Cl + M \quad (22)$$

is unlikely since $C_4F_9C(O)H$, has not been observed in the Cl + $C_4F_9CH{=}CH_2$ system. Therefore, the oxy radical most likely reacts with O_2:

$$C_4F_9CH(O)CH_2Cl + O_2 \rightarrow C_4F_9C(O)CH_2Cl + HO_2 \quad (23)$$

Some experiments carried out in pure oxygen did not show any difference in the product distribution and yields. This supports the assumption that oxy radicals predominantly react with O_2 in air.

Then, the unknown carbonyl compound detected by FTIR would be the ketone $C_4F_9C(O)CH_2Cl$.

The present results show evidence for a difference in the behavior of β-hydroxyoxy-$C_4F_9CH(O)CH_2OH$, and β-chlorooxy-$C_4F_9CH(O)CH_2Cl$ radicals. The first one would predominantly decompose whereas the second one would react with O_2. A similar behavior has already been observed for the $HOCH_2CH_2O$ and $ClCH_2CH_2O$ radicals produced in the OH- and Cl-initiated oxidation of ethene in air, respectively. The different behavior of $HOCH_2CH_2O$ and $ClCH_2CH_2O$ radicals was consistent with the higher activation barrier for decomposition of $ClCH_2CH_2O$, 15−16 kcal mol^{-1}, compared to that of $HOCH_2CH_2O$, 10−11 kcal mol^{-1}.[14] A comparable difference in the activation barrier for decomposition of $ClCH_2CH(O)CH_3$ and $OHCH_2CH(O)CH_3$ has been obtained from quantum calculations for $ClCH_2CH(O)CH_3$[15] and $HOCH_2CH(O)CH_3$.[16] Current quantum calculations from our laboratory for $ClCH_2CH(O)CF_3$ and $HOCH_2CH(O)CF_3$ lead to the same conclusion.[15] Therefore, similar difference in the activation barriers for decomposition of the $C_4F_9CH(O)CH_2Cl$ and $C_4F_9CH(O)CH_2OH$ oxy radicals is expected. This difference can explain the mechanism suggested in this work, i.e., decomposition of $HOCH_2CH(O)CF_3$ and reaction of $ClCH_2CH(O)CF_3$ with O_2.

Concerning the ketone $C_4F_9C(O)CH_2Cl$ produced in reaction 23, the two potential loss processes are photolysis and reaction with Cl. Photolysis is certainly negligible since photolysis of another chloroketone, chloroacetone, $CH_3C(O)CH_2Cl$, has been found to be negligible under the same experimental conditions as those used for the study of the Cl oxidation of $C_4F_9CH{=}CH_2$. Then, the Cl reaction is likely to be the major loss process of $C_4F_9C(O)CH_2Cl$. But the observed profiles of product concentration versus $C_4F_9CH{=}CH_2$ consumed, specially the delay in producing significant CO and COF_2 end products, indicates that the ketone is quite unreactive. Considering the existing rate constant data for Cl reaction with acetone and chloroacetone ($k = (3.1 \pm 0.4) \times 10^{-12}$ and $k = (3.5 \pm 0.4) \times 10^{-12}$ cm^3 molecule^{-1} s^{-1} at 298 K),[17] the expected rate constant for the Cl reaction with $C_4F_9C(O)CH_2Cl$ should be not higher than 2×10^{-12} cm^3 molecule^{-1} s^{-1}. The value of this rate constant will be in any case much lower than that of the initial reaction of Cl with $C_4F_9CH{=}CH_2$ ($k = (8.9 \pm 0.6) \times 10^{-11}$ cm^3 molecule^{-1} s^{-1}) and this can explain the observed product profiles.

(b) In the Presence of NO_x. Two experiments were performed with the following initial concentrations: $[HFC]_0 = 20$ and 40 ppm, $[Cl_2]_0 = 75$ and 100 ppm, and $[NO]_0 = 50$ and 150 ppm, respectively. The residual spectra obtained after subtraction of those of HFC, COF_2, and NOCl (formed through Cl + NO (+M) → ClNO (+M)) from the spectrum obtained after 60 min of irradiation time exhibit bands corresponding to PAN-like compound(s) (i.e., 1841, 1741, 1304, and 1163 cm^{-1}) as observed for the OH-initiated oxidation of $C_4F_9CH{=}CH_2$ in the presence of NO_x.

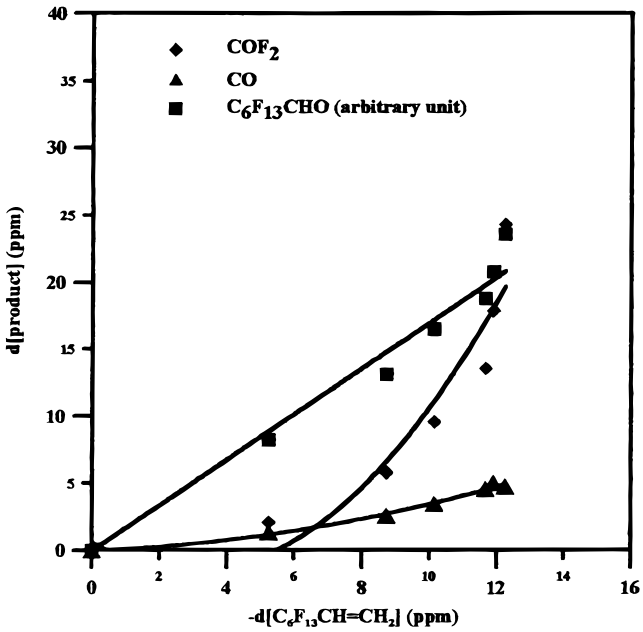

Figure 7. Concentration of product versus consumption of $C_6F_{13}CH{=}CH_2$ in the OH oxidation of $C_6F_{13}CH{=}CH_2$ in air, in the absence of NO_x, $[C_6F_{13}CH{=}CH_2]_0 = 71$ ppm.

Mechanism of the OH-Initiated Oxidation of $C_6F_{13}CH{=}CH_2$. As for $C_4F_9CH{=}CH_2$, the oxidation of $C_6F_{13}CH{=}CH_2$ was initiated either by OH or Cl in the presence and absence of NO_x. The study of $C_6F_{13}CH{=}CH_2$ is not described in detail since its oxidation mechanisms are very similar to those of $C_4F_9CH{=}CH_2$.

(a) In the Absence of NO_x. Two experiments were performed with 50 and 71 ppm of $C_6F_{13}CH{=}CH_2$. The resulting concentration profiles of the reaction products versus consumed $C_6F_{13}CH{=}CH_2$ are shown in Figure 7. In addition to CO, COF_2, and HC(O)OH, the fluorinated aldehyde ($C_6F_{13}CHO$) was observed. This latter was identified by comparison with the IR spectra obtained from the reaction of Cl with $C_6F_{13}CH_2OH$ in air which was shown to produce $C_6F_{13}CHO$ with a yield close to 100% in this laboratory. The spectra of $C_6F_{13}CHO$ were recorded from an independent experiment after 2 min irradiation of a mixture of 93 ppm of $C_6F_{13}CH_2OH$ and 96 ppm of Cl_2 in air. In Figure 8 are shown the spectrum of $C_6F_{13}CH_2OH$ (a), the spectrum obtained after 2 min irradiation of $C_6F_{13}CH_2OH/Cl_2$/air mixture (b), and the spectrum (c) resulting from subtraction of $C_6F_{13}CH_2OH$ and COF_2 from spectrum (b). The spectrum (c) is then that of $C_6F_{13}CHO$. The spectra assigned to $C_6F_{13}CHO$ and C_4F_9CHO obtained in reactions OH + $C_6F_{13}CH{=}CH_2$ and OH + $C_4F_9CH{=}CH_2$, respectively, are presented in (d) and (e). Spectra in (c), (d), and (e) show that the position of the absorption band centered at 1778 cm^{-1}, due to the C=O group of the aldehyde is not affected by the number of the surrounding C−F bonds (C_4F_9 or C_6F_{13}).

The profiles shown in Figure 7 indicate that $C_6F_{13}CHO$ is a primary product of the reaction while CO and COF_2 are secondary products as observed for $C_4F_9CH{=}CH_2$. The overall oxidation mechanism of $C_6F_{13}CH{=}CH_2$ is expected to be similar to that for $C_4F_9CH{=}CH_2$.

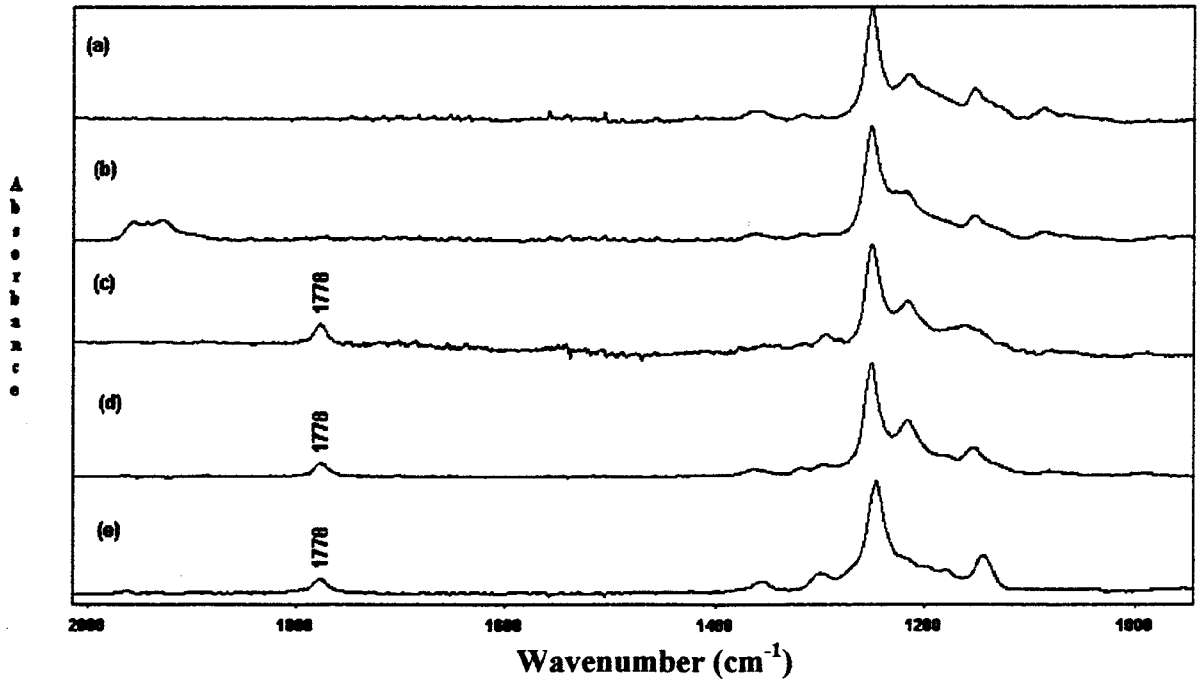

Figure 8. FTIR spectra for the Cl + $C_6F_{13}CH_2OH$ reaction in air, in the absence of NO_x: **(a)** spectrum of $C_6F_{13}CH_2OH$ before irradiation, **(b)** spectrum after 2 min irradiation, **(c)** spectrum of $C_6F_{13}CHO$ after subtraction of $C_6F_{13}CH_2OH$ and COF_2, **(d)** spectrum of $C_6F_{13}CHO$ from the OH + $C_6F_{13}CH{=}CH_2$ reaction, and **(e)** spectrum of C_4F_9CHO from the OH + $C_4F_9CH{=}CH_2$ reaction.

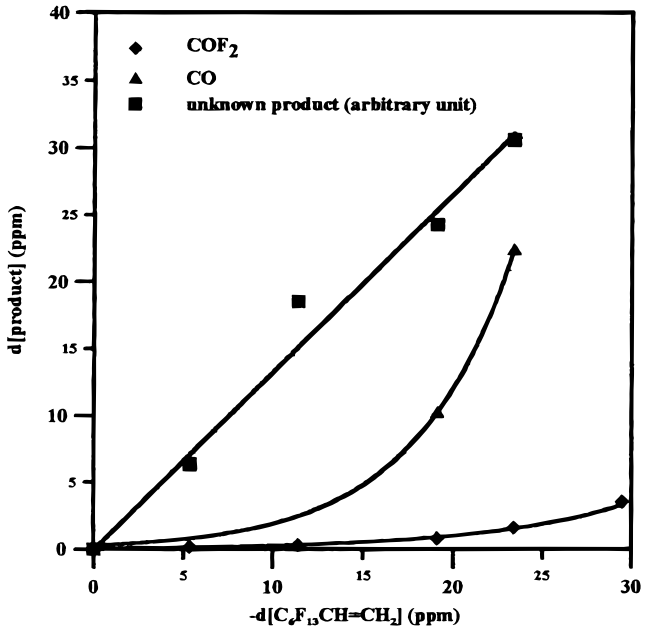

Figure 9. Concentrations of products versus consumption of $C_6F_{13}CH{=}CH_2$ in the Cl oxidation of $C_6F_{13}CH{=}CH_2$ in air, in the absence of NO_x, $[C_6F_{13}CH{=}CH_2]_0$ = 30 ppm.

(b) In the Presence of NO_x. Two experiments were conducted with the initial concentrations $[C_6F_{13}CH{=}CH_2]_0$ = 50 and 71 ppm, and $[NO]_0$ = 25 and 140 ppm, respectively. CO, HC(O)OH, and COF_2 were identified as products. Characteristic bands of a PAN-like compound were also observed, as in the OH + $C_4F_9CH{=}CH_2$ experiments in the presence of NO_x.

Mechanism of the Cl-Initiated Oxidation of $C_6F_{13}CH{=}CH_2$. *(a) In the Absence of NO_x.* Two experiments were performed with the initial concentrations $[C_6F_{13}CH{=}CH_2]_0$ = 15 and 30 ppm, and $[Cl_2]_0$ = 150 and 30 ppm, respectively. The profiles of the reaction products versus $C_6F_{13}CH{=}CH_2$ consumed are shown in Figure 9. As in the $C_4F_9CH{=}CH_2$ experiments, the profiles of CO and COF_2 behave like that of secondary products, and the spectrum of the intermediate product differs slightly from that of the fluorinated aldehyde ($C_6F_{13}CHO$).

One experiment was conducted in pure O_2 ($[C_6F_{13}CH{=}CH_2]_0$ = 32 ppm, $[Cl_2]_0$ = 60 ppm). The resulting profiles of the products were similar to that in air, indicating that the nature of the products and their yields do not depend on the concentration of O_2. This suggests, similarly to the Cl + $C_4F_9CH{=}CH_2$ mechanism, that the oxy radical $C_6F_{13}CH(O)CH_2Cl$ expected to be formed reacts predominantly with O_2, the decomposition being negligible. The expected reaction product is the ketone, $C_6F_{13}C(O)CH_2Cl$, corresponding to the unknown carbonyl infrared band observed.

(b) In the Presence of NO_x. A single experiment was conducted where the initial concentrations of $C_6F_{13}CH{=}CH_2$, Cl_2, and NO were 31, 90, and 60 ppm, respectively. The reaction product profiles (CO, COF_2, and an unknown product with a band at 1788 cm^{-1}) are similar to those obtained with $C_4F_9CH{=}CH_2$.

Conclusion

The results from this work provide some additional information concerning the behavior of β-hydroxy-oxy and β-chloro-oxy radicals, produced in OH and Cl oxidation of alkenes in air. The obtained results suggest that the $C_4F_9CH(O)CH_2OH$ (and $C_6F_{13}CH(O)CH_2OH$) oxy radicals will decompose, whereas the $C_4F_9CH(O)CH_2Cl$ (and $C_6F_{13}CH(O)CH_2Cl$) oxy radicals will react with O_2 under air conditions. Such a different behavior of β-hydroxyoxy and β-chlorooxy radicals, previously observed for $HOCH_2CH_2O$ and $ClCH_2CH_2O$,[14] can be explained by a significantly higher activation barrier for decomposition of the β-chlorooxy compared to that for the decomposition of the β-hydroxyoxy radicals. This different behavior leads to different oxidation products since aldehydes will be produced in the OH oxidation and ketones in the Cl oxidation of alkenes (except ethene). This will have atmospheric implications if both OH and Cl oxidation of alkenes occur in the atmosphere.

Concerning the atmospheric implications of this work, the obtained results provide some information about the atmospheric fate and impact of the studied HFCs if such compounds would be used for industrial applications and released to the atmosphere. Although the rate constants of the Cl reactions with the studied HFCs are about 60 times higher than that of the OH reactions, the OH reaction is very likely to be predominant in the atmosphere, considering the assumed [Cl]/[OH] atmospheric ratio (typically 10^3 cm^{-3}/10^6 cm^{-3} $\approx$ 10^{-3}). Therefore, the atmospheric lifetimes of $C_4F_9CH{=}CH_2$ and $C_6F_{13}CH{=}CH_2$ would be around 8 days. This low lifetime first implies that these HFCs would have a negligible greenhouse effect although they strongly absorb infrared radiation in the atmospheric window, as all the fluorine-containing hydrocarbons. Then the rather short-lived $C_4F_9CH{=}CH_2$ and $C_6F_{13}CH{=}CH_2$ could have a local or regional impact. Since they would be oxidized under "rich" NO_x conditions, they can produce ozone. Their ozone-forming potential will depend on the fate of the intermediate carbonyl compound, C_4F_9CHO and $C_6F_{13}CHO$, which is still poorly known. The rates of their OH reaction and photolysis need to be determined. The fate of these carbonyl compounds will also influence the fluorinated product distribution and impact. The OH reaction may lead to stable PAN type compounds ($C_4F_9C(O)O_2NO_2$ and $C_6F_{13}C(O)O_2NO_2$) while photolysis is likely to produce COF_2 molecules by oxidation of the C_4F_9 and C_6F_{13} photofragments.

Acknowledgment. We thank Elf Atochem Co. and Conseil Régional du Centre for providing research grants to E.V.

References and Notes

(1) Mellouki, A.; Téton, S.; Le Bras, G. *Int. J. Chem. Kinet.* **1995**, *27*, 791.

(2) Mellouki, A.; *J. Chim. Phys.* **1998**, *95*, 503.

(3) Porter, E.; Wenger, J.; Treacy, J.; Sidebottom, H.; Mellouki, A.; Téton, S.; Le Bras, G. *J. Phys. Chem.* **1997**, *101*, 5770.

(4) Orkin, V. L.; Huie, R. E.; Kurylo, M. *J. Phys. Chem. A* **1997**, *101*, 9118.

(5) Kaiser, E. W.; Wallington, T. J. *J. Phys. Chem.* **1996**, *100*, 9788.

(6) Cvetanovic, R. J. Presented at the 12th International Symposium On Free Radicals, Laguna Beach, CA, January 4−9, 1976.

(7) Veyret, B.; Lesclaux, R.; Rayez, M.-T.; Rayez, J.-C.; Cox, R. A.; Moortgat, G. K. *J. Phys. Chem.* **1989**, *93*, 2368.

(8) Anderson, L. R.; Fox, W. B. *J. Am. Chem. Soc.* **1967**, *89*, 4313.

(9) Hirschmann, R. P.; Fox, W. B.; Anderson, L. R. *Spectrochim. Acta* **1969**, *25A*, 811.

(10) Scollard, D. J. Ph.D. Thesis, University College Dublin, 1992.

(11) Scollard, D. J.; Treacy, J. J.; Sidebottom H. W.; Balestra-Garcia, C.; Laverdet, G.; Le Bras, G.; MacLeod, H.; Téton, S. *J. Phys. Chem.* **1993**, *97*, 4683.

(12) Chen, J.; Zhu, T.; Niki, H. *J. Phys. Chem.* **1992**, *96*, 6115.

(13) Chen, J.; Young, V.; Zhu, T.; Niki, H. *J. Phys. Chem.* **1993**, *97*, 11696.

(14) Orlando, J. J.; Tyndall, G. S.; Bilde, M.; Ferronato, C.; Wallington, T. J.; Vereeken, L.; Peeters, J. *J. Phys. Chem. A* **1998**, *102*, 8116.

(15) Kukui, A., private communication.

(16) Vereeken, L.; Peeters, J.; Orlando, J. J.; Tyndall, G. S.; Ferronato, C. *J. Phys. Chem. A.* 1999, *103*, 4693.

(17) Notario, A.; Mellouki, A.; Le Bras, G. *Int. J. Chem. Kinet*. 2000, *32*, 63.